ACS Macro Letters

Letter

pubs.acs.org/macroletters

Facile Synthesis of Stable and Water-Dispersible Multihydroxy Conjugated Polymer Nanoparticles with Tunable Size by Dendritic Cross-Linking

Li Zhou, Junlong Geng, Guan Wang, Jie Liu, and Bin Liu*

Department of Chemical and Biomolecular Engineering, National University of Singapore, 4 Engineering Drive 4, 117576, Singapore

Supporting Information

ABSTRACT: A new strategy has been developed to synthesize conjugated polymer (CP) nanoparticles (CPNs) with numerous surface hydroxyl groups via click chemistry between a CP and hyperbranched polyglycerol (HPG) in miniemulsion. Laser light scattering and TEM characterizations indicate that the synthesized CPNs have spherical shapes with uniform sizes tunable in the range of 40−210 nm simply by adjusting the feed amount of the oil phase or surfactant in the miniemulsion. The obtained CPNs have good water dispersibility and orange emission with high fluorescence quantum yields of 23 ± 2%. Detailed spectroscopy studies reveal that the CPNs have shown stable fluorescence against pH change, ionic strength variation, or protein disturbance. In addition, they have good photostability and low cytotoxicity, which make them an ideal fluorescent moiety for cellular imaging. This study provides important fundamental understanding of cross-linking modification on CP to form CPNs, which will stimulate further research on synthesis and application of advanced CPNs.

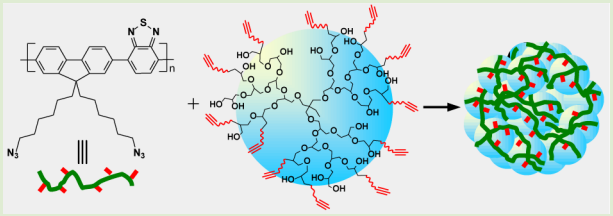

The development of fluorescent bioimaging reagents has gained significant attention in recent years. An ideal bioimaging reagent generally requires high fluorescence quantum yield (QY), good optical stability, biocompatibility, and surface functionality.[1] As a promising candidate, conjugated polymers (CPs) have shown advantages over small fluorophores, fluorescent proteins, and even semiconductor quantum dots (QDs), which include large absorption cross sections, bright fluorescence, and favorable biocompatibility.[2] However, CPs with inherent hydrophobic backbones are insoluble in water. As a consequence, it is highly desirable to endow CPs with good water dispersibility to facilitate their biological applications.

Several strategies have been developed to transform organic soluble CPs into aqueous media, which include emulsion technique, precipitation technique, design and synthesis of conjugated polyelectrolytes (CPEs) and direct polymerization in heterophase system.[3] Among them, synthesis of CPEs and formation of CP nanoparticles (CPNs) via precipitation technique are the two most widely used strategies. However, the synthesis of CPEs generally requires laborious synthetic steps and the modification has to be specifically designed for each CP. In addition, the charged side chains of CPEs often lead to nonspecific interactions with biomolecules.[4] The other commonly employed strategy is to form CP nanoparticles (CPNs) by precipitation technique in the absence or presence of surfactants.[5] It involves the dissolution of CPs in organic solvents, followed by injection of the CP solutions into water with ultrasonication. CPNs are formed when hydrophobic CP chains fold into spherical shape to release interface energy. A variety of water-dispersible CPNs have been synthesized via this approach, however, these CPNs with hydrophobic surface are not inherently stable, and their surface possesses no functional groups for further functionalization.[6] Recently, embedding CPs into polymer matrix such as carboxylic polyethylene glycol and poly(DL-lactide-*co*-glycolide) afforded CPNs with surface functional groups.[7,8] The poor structural stability resulted from noncovalent interaction may cause microphase separation or CP leakage, which is problematic for practical applications.[8,9] As the polymer encapsulated CPNs generally have −COOH or $-NH_2$ functional groups, they could also lead to undesired association with cell membrane and other charged biomolecules via hydrophobic and electrostatic interactions.[7−10] Despite the progress on CPNs in recent years, the preparation of CPNs with inherent hydrophilic surface, multiple neutral functional groups, and high structural stability is still in its infancy.

In this contribution, we report a new strategy toward water-dispersible CPNs via copper-free click chemistry in an oil-in-water miniemulsion system, as shown in Scheme 1. Hyperbranched polyglycerol (HPG) was selected as the cross-linker because it is a well-known biocompatible dendritic polymer with good water solubility and numerous reactive hydroxyl groups.[11] In addition, HPG can be easily synthesized by one-step polymerization as compared to dendrimers.[12] As one of the most widely used CPs for CPN formation, poly[9,9′-dihexylfluorene-*coalt*-4,7-(2,1,3-benzothiadiazole)] (PFBT) was chosen as a representative CP to react with HPG.[7−10] Detailed studies reveal that the cross-linked CP−HPG nanoparticles

Received: June 6, 2012
Accepted: July 3, 2012
Published: July 10, 2012

Scheme 1. Schematic Illustration of the Preparation of CP−HPG Nanoparticles

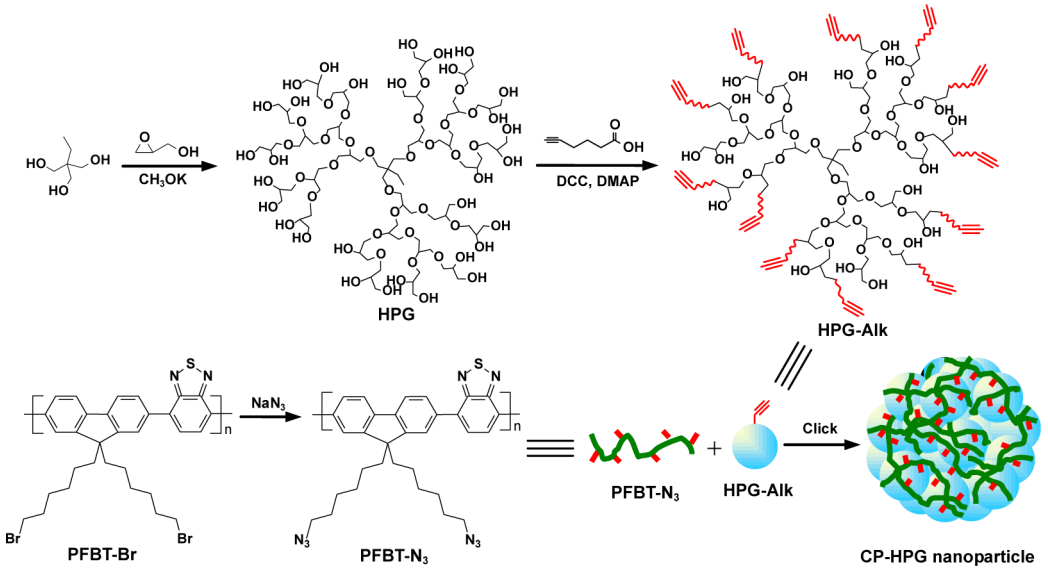

with multiple surface hydroxy groups exhibit good structural stability and water dispersibility, high fluorescence QY, stable optical properties, and low cytotoxicity. In addition, CP−HPG nanoparticles show tunable size in the range of 40−210 nm with narrow size distribution, simply by adjusting the oil phase and surfactant used for miniemulsion. This work opens a new opportunity to synthesize functional water-dispersible fluorescent CPNs.

The synthetic route to water-dispersible CPNs is depicted in Scheme 1. Poly[9,9′-bis(6″-bromohexyl)fluorene-*coalt*-4,7-(2,1,3-benzothiadiazole)] (PFBT−Br, M_n = 15000, polydispersity (PDI) = 1.75) was synthesized according to our previous report.[13] The −Br groups were then transformed to $-N_3$ groups by reaction between PFBT−Br and sodium azide to afford poly[9,9′-bis(6″-azidohexyl)fluorene-*coalt*-4,7 -(2,1,3-benzothiadiazole)] (PFBT−N_3) in 95% yield. After the reaction, the resonance peaks at around 3.30 ppm for $-CH_2Br$ disappears and new peaks appear at 3.18 ppm for $-CH_2N_3$ in the ^{1}H NMR spectrum for PFBT−N_3, indicating the successful transformation of −Br to $-N_3$. This is further verified by the appearance of an obvious peak at 2104 cm^{-1} corresponding to $-N_3$ groups in the FTIR spectrum of PFBT−N_3 (Figure 1).

HPG (M_n = 15500, PDI = 1.23) was synthesized by anionic ring-opening polymerization according to the literature,[14] which has excellent water solubility. The structure of HPG was characterized by FTIR and NMR spectra (Figure 1, Figures S1 and S2 in the Supporting Information, SI). The degree of branching (DB) for the HPG calculated from the results of inverse-gated ^{13}C NMR spectrum is about 0.53 (Figure S2 in the SI).[15] The surface hydroxyl groups of HPG were subsequently esterified with 5-hexynoic acid (HA) in the presence of *N*,*N*′-dicyclohexylcarbodiimide (DCC) to afford alkyne-modified HPG (HPG−Alk). As compared to the FTIR spectrum of HPG, two new peaks at 2105 and 1724 cm^{-1} corresponding to −C≡CH and −C═O groups appear on the FTIR spectrum for HPG−Alk. In addition, the resonance peaks at 2.27 ppm ($-C\underline{H}_2C{\equiv}CH$), 2.0 ppm ($-C{\equiv}C\underline{H}$), and 1.85 ppm ($-C\underline{H}_2CH_2C{\equiv}CH$) in the ^{1}H NMR spectrum of HPG−Alk also suggest its right structure (Figure S3 in the SI). The conversion efficiency of the hydroxyl groups to alkyne groups

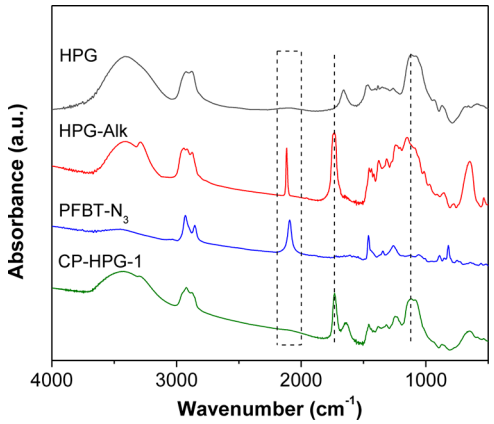

Figure 1. FT-IR spectra of HPG, HPG−Alk, PFBT−N_3, and CP−HPG-1.

calculated from the ^{1}H NMR spectra of HPG and HPG−Alk is ∼20%, which is further confirmed by the GPC result of HPG−Alk (M_n = 19200, PDI = 1.32) relative to HPG (Figure S4 in the SI). It should be noted that the HPG−Alk still possesses numerous hydroxyl groups (∼168 −OH groups per HPG−Alk macromolecule calculated from the GPC and NMR results). The HPG−Alk shows good solubility in organic solvents such as dichloromethane and chloroform but is not dispersible in water. The detailed synthesis and characterization are shown in the SI. Similar to HPG−Alk, HPG−Alk2 (M_n = 35600, PDI = 1.20) with over 80% surface alkyne groups was also synthesized simply by increasing the feed ratio of HA to HPG.

As copper ions are toxic to biosubstrates, biocompatible copper-free click coupling was adopted to synthesize CP−HPG nanoparticles using thermal initiation in oil-in-water miniemulsion.[16] PFBT−N_3 and HPG−Alk with 1:1 azide/alkyne ratio were first dissolved in chloroform (oil phase) and then the mixture was miniemulsified with water in the presences of sodium dodecyl sulfate (SDS) surfactant. As the temperature increased to 85 °C, click reaction between HPG−Alk and PFBT−N_3 occurred. After reaction, transparent orange aqueous solution was obtained, indicating good water dispersibility of the CP−HPG nanoparticles. The disappearance of the peak at

dx.doi.org/10.1021/mz300282s | *ACS Macro Lett.* 2012, 1, 927−932

about 2100 cm^{-1} corresponding to alkyne or azide groups in the FTIR spectrum of CP−HPG confirms the nearly complete "click" cross-linking and efficient thermal initiation (Figure 1). Meanwhile, the peak at 3400 cm^{-1} remains strong, indicating that the CP−HPG nanoparticles possess numerous hydroxyl groups.

To probe the effect of miniemulsion conditions on the size of CP−HPG nanoparticles, we conducted a series of experiments by changing the feed ratio of oil phase or surfactant to water (Table 1). The sizes of the obtained CP−HPG nanoparticles were investigated by laser light scattering (LLS), and the results are shown in Figure 2a and Figure S5 in the SI. As the critical micelle concentration (CMC) for SDS in water is about 8.0 mM, we first fixed the concentration of SDS (C_{SDS}) at 9.5 mM. The size of CP−HPG nanoparticles increased from 83 to 152 nm with increased oil phase from 1 to 3 mL. This is due to the fact that more oil phase could result in the formation of bigger micelles at the same C_{SDS} in an oil-in-water system.[17] On the other hand, it is found that at a constant oil-to-water ratio, the size of CP−HPG increased from 44 to 210 nm when the C_{SDS} was varied from 12.5 to 8.0 mM (Table1). This is consistent with previous reports on using miniemulsion to synthesize polystyrene and poly(*N*-isopropylacrylamide) nanoparticles.[18] These results indicate that the size of CP−HPG nanoparticles could be fine-tuned simply by adjusting the oil phase and surfactant used in the miniemulsion. All the CP−HPG nanoparticles synthesized with SDS as the surfactant showed narrow size distribution (PDI < 0.07) and good water dispersibility. Transmission electron microscopy (TEM) further verified the well-defined nanostructure and uniform size. As shown in Figure 2b, the CP−HPG-1 nanoparticles exhibit spherical shape with an average size of 78 nm, which is slightly smaller than that for LLS data (Table 1).

Table 1. Reaction Parameters and the Optical Properties of the Water-Dispersible CP−HPG Nanoparticles[a]

product	$V_{oil\ phase}$ (mL)	C_{SDS} (mM)	diameter[b] (nm)	PDI[b]	QY
CP−HPG-1	1	9.5	83	0.046	0.24
CP−HPG-2	2	9.5	114	0.053	0.23
CP−HPG-3	3	9.5	152	0.048	0.21
CP−HPG-4	1	12.5	44	0.042	0.25
CP−HPG-5	1	8.0	210	0.068	0.21
CP−HPG-6	1	0	135	0.723	0.17

[a]Volume of the water phase is 20 mL. The feed amounts of PFBT−N_3 and HPG−Alk are 11.8 and 7 mg, respectively; [azide]/[alkyne] = 1:1. [b]Determined by LLS.

It is worth noting that both the HPG−Alk and the PFBT−N_3 have good solubility in chloroform. Interestingly, after click reaction, the products show good dispersibility in water phase (Figure S6 in the SI). The SDS surfactant should be removed by repeated washing with hexane, followed by dialysis against Milli-Q water for five days. We deduce that the good water dispersibility of the CP−HPG nanoparticles is attributed to the presence of numerous hydrophilic hydroxyl groups on the surface of CP−HPG nanoparticles while the hydrophobic domain is encapsulated as the core after the click reaction. To prove this conjecture, first, a control experiment for CP−HPG-6 in the absence of SDS was conducted (Table 1). The resulted CP−HPG-6 presents good dispersibility in the upper aqueous layer of a water/chloroform mixture, which indicates that SDS is not directly related to water dispersibility of the CP−HPG nanoparticles, although it significantly affects the nanoparticle size and morphology (Figure S7 in the SI). In addition, HPG−Alk2 was also reacted with PFBT−N_3 (1:1 alkyne/azide) in miniemulsion and the product showed good dispersibility in water. However, when HPG−Alk2 with 4:1 alkyne/azide was used, the resulting CP−HPG nanoparticles exhibited amphibious dispersibility that can be dispersed both in water and in chloroform phase as a result of the presence of hydroxyl groups and un-cross-linked HA chains on their surface. Based on these results, the good water dispersibility of the CP−HPG nanoparticles is attributed to the presence of numerous hydrophilic neutral hydroxyl groups on the surface of CP−HPG nanoparticles. These results also suggest that the surface functionality of CP−HPGs can be easily fine-tuned by choosing suitable cross-linkers.

The absorption and emission spectra of CP−HPG-1 nanoparticles in aqueous solution are shown in Figure 2c. Compared with the PFBT−N_3 in dichloromethane, no obvious shift is observed for the absorption and emission peaks of the CP−HPG-1. All the CP−HPG nanoparticles prepared using SDS as surfactant exhibit strong fluorescence with quantum yields (QYs) higher than 20% (Table 1), which compare favorably to other reported CPNs based on PFBT with QYs less than 10%.[10,19] Such a high fluorescence QY of CP−HPG nanoparticles could be attributed to the minimized self-quenching of PFBT in the CPNs format. As compared to the CPNs prepared by the precipitation approach, the introduction of HPG as a spherical scaffold to the polymer side chain can effectively reduce the chain tangling and $\pi-\pi$ stacking of CPs, leading to reduced polymer fluorescence self-quenching.

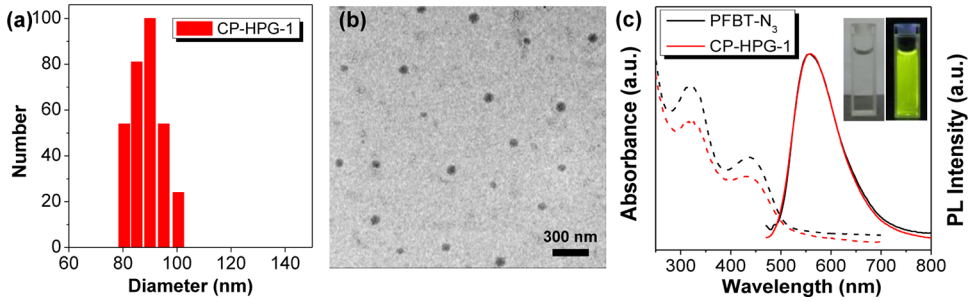

Figure 2. Hydrodynamic radius distribution (a) and TEM image (b) of CP−HPG-1. UV−vis absorption (dashed line) and emission (solid line) spectra (c) of PFBT−N_3 in dichloromethane and CP−HPG−1 in aqueous solution (λ_{ex} = 450 nm). The inset of (c) is the aqueous solution of CP−HPG-1 nanoparticles under daylight (left) and 365 nm UV light illumination (right).

dx.doi.org/10.1021/mz300282s | *ACS Macro Lett.* 2012, 1, 927−932

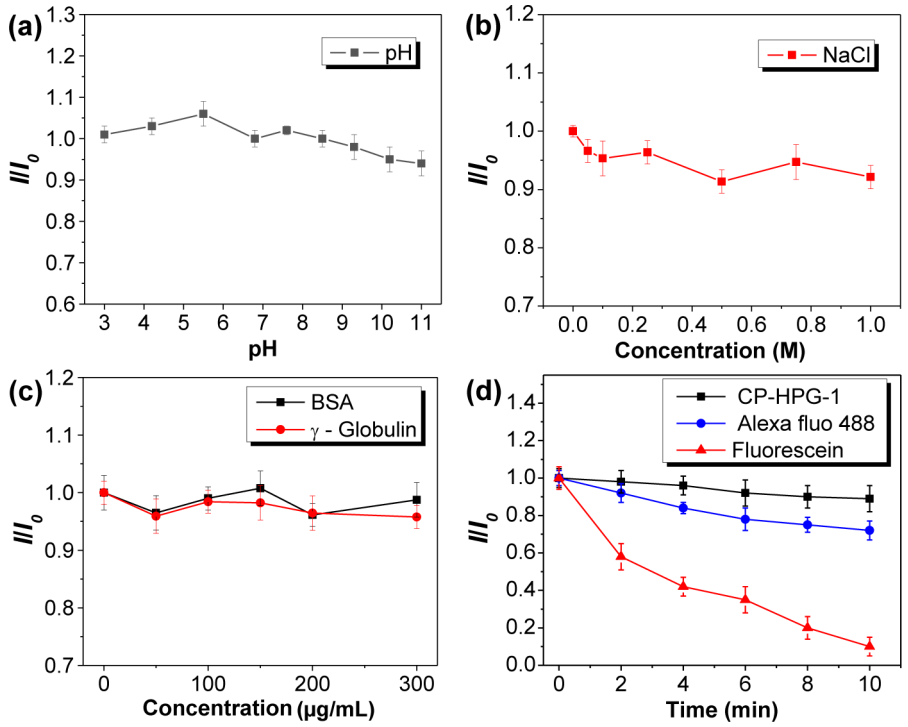

Figure 3. pH (a), NaCl concentration (b), BSA, and γ-globulin concentration (c) dependent fluorescence intensity ratio (I/I_0). For (a), (b), and (c), I_0 is the emission intensity of CP−HPG-1 aqueous solution in the absence of NaCl, BSA, and γ-globulin, I is the emission intensity of CP−HPG-1 aqueous solution at different pH values (a) or different concentrations of NaCl (b), BSA, and γ-globulin (c). Illumination time-dependent fluorescence intensity ratio (I/I_0) of CP−HPG-1, Alexafluo 488, and fluorescein (d). I_0 and I are the emission intensities of CP−HPG-1, Alexafluo 488 and fluorescein without and with illumination for different time, respectively. The concentrations of CP−HPG-1 for (a), (b), and (c) are at [RU] = 20 μM, and for (d) is at [RU] = 1 μM.

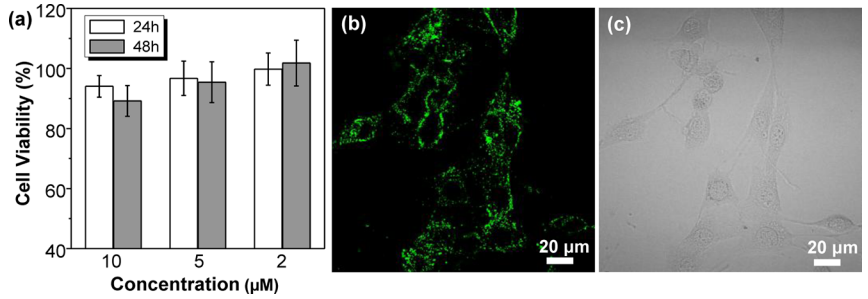

Figure 4. (a) Cell viability of MCF-7 cells after incubation with CP−HPG-1 at different concentrations for 24 and 48 h, respectively. Confocal fluorescence image (b) and bright-field image (c) of MCF-7 cells upon incubation with CP−HPG-1 ([RU] = 1 μM) for 2 h.

Therefore, using HPG as cross-linker can not only endow CPs with hydrophilic neutral hydroxy groups associated with good water dispersibility but also can retain strong fluorescence of the CPs.

Considering the complex physiological environment for bioimaging applications, the physical stability of CP−HPG nanoparticles in aqueous solution was examined under different conditions. Because all the CP−HPG nanoparticles show similar optical properties, CP−HPG-1 was chosen as a representative for the following studies. The concentration of CP−HPG-1 solution was calculated based on the concentration of PFBT repeat unit (RU). The fluorescence change of CP−HPG-1 at [RU] = 20 μM and different pH is shown in Figure 3a. Less than 5% variation in emission intensity is observed when the pH is changed from 3 to 11. In addition, there is very little fluorescence change when the solution ionic strength is increased from 0 to 1 M (Figure 3b). This compares favorably to CPEs and other CPNs with a charged surface that show obvious fluorescence quenching in solutions with relatively high ionic strength.[20] In addition, the CP−HPG-1 possesses high colloidal stability in water and no obvious precipitate is observed even after being stored at room temperature for three months.

As proteins largely exist in biological media, BSA and γ-globulin (a kind of immunoglobulin in blood) were chosen as the representative examples to study their interactions with CP−HPG-1. As shown in Figure 3c, the CP−HPG-1 fluorescence remains unchanged when the protein concentrations are increased from 0 to 300 μg/mL. LLS measurements further confirm that there is no significant difference in size and size distribution of CP−HPG-1 in aqueous solution before and after the addition of BSA and γ-globulin, suggesting good antiprotein adsorption property of CP−HPG-1. In addition, the photostability of CP−HPG-1 was studied by continuous

dx.doi.org/10.1021/mz300282s | ACS Macro Lett. 2012, 1, 927−932

imaging using confocal laser scanning microscopy (CLSM) for 10 min. For comparison, commercially available fluorescent dyes such as Alexafluo 488 and fluorescein were also investigated under the same condition. As shown in Figure 3d, the emission intensities decrease by 11, 28, and 90% at 10 min for CP−HPG-1, Alexafluo 488, and fluorescein, respectively. These studies indicate that the CP−HPG-1 nanoparticles possess good physical and photo stabilities, which make them good candidates for biological applications.

The cytotoxicity of CP−HPG-1 was evaluated for MCF-7 breast cancer cells using MTT cell-viability assay. Figure 4a summarizes the in vitro MCF-7 cell viability after being cultured for 24 or 48 h. It is noteworthy that the concentrations of the CP−HPG-1 solution are much higher than that used for cell imaging ([RU] = 1 μM). The cell viabilities are close to 100% at [RU] = 2 and 5 μM and close to 90% at [RU] = 10 μM within the tested period, suggesting the low cytotoxicity of CP−HPG-1. This result is consistent with the previous studies of CPNs prepared by precipitation technique.[8] The good biocompatibility of CP−HPG-1 should also benefit from the highly biocompatible HPG.

To demonstrate the CP−HPG nanoparticles in cell imaging, MCF-7 cells were incubated with CP−HPG-1 solution at [RU] = 1 μM. After a 2 h incubation, the cells were fixed for fluorescence imaging by CLSM. The excitation wavelength was fixed at 488 nm, and the fluorescent signals were collected above 540 nm. The CLSM image of CP−HPG-1 stained MCF-7 cells is displayed in Figure 4b. Strong fluorescence from the cellular cytoplasm is observed for MCF-7 cells, implicating that CP−HPG-1 is efficiently internalized by MCF-7 cells and accumulated in the cytoplasm, which is further confirmed by the 3D CLSM image (Figure S8 in the SI). In contrast, no fluorescence can be observed for the cells without incubation of CP−HPG-1 (Figure S9 in the SI). These data suggest that CP−HPG-1 can be used as an effective fluorescent stain for cell imaging with good fluorescence contrast.

In summary, we have successfully demonstrated a simple and effective approach to fabricate robust CP−HPG nanoparticles via copper-free click reaction in oil-in-water miniemulsion. The CP−HPG nanoparticles with tunable size are born with multiple surface neutral hydroxyl groups, which have shown good water dispersibility, bright fluorescence, good optical stability, and low cytotoxicity. As the first example to combine dendritic polymer and CP by covalent cross-linking, this study not only exploits a new type of CPN with desired properties, but also provides new opportunities and fundamental guidelines to design advanced CPNs for biological applications.

■ ASSOCIATED CONTENT

Ⓢ Supporting Information

Detailed experimental procedures, NMR spectra, and GPC curves of HPG−Alk, additional LLS and TEM results of CP−HPG, 3D confocal fluorescence image, and control confocal image of MCF-7 cells. This material is available free of charge via the Internet at http://pubs.acs.org.

■ AUTHOR INFORMATION

Corresponding Author

*E-mail: cheliub@nus.edu.sg.

Notes

The authors declare no competing financial interest.

■ ACKNOWLEDGMENTS

The authors are grateful to the Singapore National Research Foundation (R279-000-323-281), the Temasek Defence Systems Institute (R279-000-305-232/422/592), and Singapore Defense Innovative Research Programme (R279-000-340-232) for financial support.

■ REFERENCES

(1) (a) Naczynski, D. J.; Andelman, T.; Pal, D.; Chen, S.; Riman, R. E.; Roth, C. M.; Moghe, P. V. *Small* **2010**, *6*, 1635−1639. (b) Grunwald, C.; Schulze, K.; Giannone, G.; Cognet, L.; Lounis, B.; Choquet, D.; Tampé, R. *J. Am. Chem. Soc.* **2011**, *133*, 8090−8093. (c) Duarte, A.; Pu, K. Y.; Liu, B.; Bazan, G. C. *Chem. Mater.* **2011**, *23*, 501−515.

(2) (a) Thomas, S. W., III; Joly, G. D.; Swager, T. M. *Chem. Rev.* **2007**, *107*, 1339−1386. (b) Wu, C.; Jin, Y.; Schneider, T.; Burnharm, D. R.; Smith, P. B.; Chiu, D. T. *Angew. Chem., Int. Ed.* **2010**, *49*, 9436−9440. (c) Rahim, N. A. A.; McDaniel, W.; Bardon, K.; Srinivasan, S.; Vickerman, V.; So, P. T. C.; Moon, J. H. *Adv. Mater.* **2009**, *21*, 3492−3496. (d) Pu, K. Y.; Liu, B. *Adv. Funct. Mater.* **2011**, *21*, 3408−3423. (e) Li, K.; Liu, B. *J. Mater. Chem.* **2012**, *22*, 1257−1264.

(3) (a) Pecher, J.; Mecking, S. *Chem. Rev.* **2010**, *110*, 6260−6279. (b) Kelly, T. L.; Wolf, M. O. *Chem. Soc. Rev.* **2010**, *39*, 1526−1535. (c) Pinto, M. R.; Schanze, K. S. *Synthesis* **2002**, 1293−1309. (d) Liu, B.; Bazan, G. C. *J. Am. Chem. Soc.* **2006**, *128*, 1188−1196. (e) Traina, C. A.; Bakus, R. C., II; Bazan, G. C. *J. Am. Chem. Soc.* **2011**, *133*, 12600−12607. (f) Ho, H. A.; Najari, A.; Leclerc, M. *Acc. Chem. Res.* **2008**, *41*, 168−178. (g) Liu, B.; Bazan, G. C. *Chem. Mater.* **2004**, *16*, 4467−4476. (h) Wang, Y. Y.; Liu, B. *Curr. Org. Chem* **2011**, *15*, 446−464.

(4) (a) Wosnick, J. H.; Mello, C. M.; Swager, T. M. *J. Am. Chem. Soc.* **2005**, *127*, 3400−3405. (b) Pu, K. Y.; Shi, J.; Cai, L.; Li, K.; Liu, B. *Biomacromolecules* **2011**, *12*, 2966−2974.

(5) (a) Wu, C.; McNeill, J. *Langmuir* **2008**, *24*, 5855−5861. (b) Li, K.; Liu, Y.; Pu, K. Y.; Feng, S. S.; Zhan, R.; Liu, B. *Adv. Funct. Mater.* **2011**, *21*, 287−294. (c) Park, E. J.; Erdem, T.; Ibrahimova, V.; Nizamoglu, S.; Demir, H. V.; Tuncel, D. *ACS Nano* **2011**, *5*, 2483−2492.

(6) (a) Wu, C.; Szymanski, C.; Cain, Z.; McNeill, J. *J. Am. Chem. Soc.* **2007**, *129*, 12904−12905. (b) Tuncel, D.; Demir, H. V. *Nanoscale* **2010**, *2*, 484−494. (c) Hashim, Z.; Howes, P.; Green, M. *J. Mater. Chem.* **2011**, *21*, 1797−1803. (d) Baier, M. C.; Huber, J.; Mecking, S. *J. Am. Chem. Soc.* **2009**, *131*, 14267−14273.

(7) Wu, C.; Schneider, T.; Zeigler, M.; Yu, J.; Schiro, P. G.; Burnham, D. R.; McNeill, J. D.; Chiu, D. T. *J. Am. Chem. Soc.* **2010**, *132*, 15410−15417.

(8) Li, K.; Pan, J.; Feng, S. S.; Wu, A. W.; Pu, K. Y.; Liu, Y.; Liu, B. *Adv. Funct. Mater.* **2009**, *19*, 3535−3542.

(9) Pecher, J.; Huber, J.; Winterhalder, M.; Zumbusch, A.; Mecking, S. *Biomacromolecules* **2010**, *11*, 2776−2780.

(10) (a) Ibrahimova, V.; Ekiz, S.; Gezici, Ö.; Tuncel, D. *Polym. Chem* **2011**, *2*, 2818−2824. (b) Kandel, P. K.; Fernando, L. P.; Ackroyd, P. C.; Christensen, K. A. *Nanoscale* **2011**, *3*, 1037−1045.

(11) (a) Wilms, D.; Stiriba, S. E.; Frey, H. *Acc. Chem. Res.* **2010**, *43*, 129−141. (b) Calderón, M.; Quadir, M. A.; Sharma, S. K.; Haag, R. *Adv. Mater.* **2010**, *22*, 190−218. (c) Kainthan, R. K.; Hester, S. R.; Levina, E.; Devine, D. V.; Brooks, D. E. *Biomaterials* **2007**, *28*, 4581−4590.

(12) Gao, C.; Yan, D. *Prog. Polym. Sci.* **2004**, *29*, 183−275.

(13) (a) Liu, B.; Bazan, G. C. *Nat. Protoc.* **2006**, *1*, 1698−1702. (b) Pu, K. Y.; Fang, Z.; Liu, B. *Adv. Funct. Mater.* **2008**, *18*, 1321−1328.

(14) (a) Kainthan, R. K.; Muliawan, E. B.; Hatzikiriakos, S. G.; Brooks, D. E. *Macromolecules* **2006**, *39*, 7708−7717. (b) Sunder, A.; Bauer, T.; Mülhaupt, R.; Frey, H. *Macromolecules* **2000**, *33*, 1330−1337. (c) Zhou, L.; Gao, C.; Hu, X.; Xu, W. *Chem. Mater.* **2011**, *23*, 1461−1470.

(15) (a) Sunder, A.; Hanselmann, R.; Frey, H.; Mülhaupt, R. *Macromolecules* **1999**, *32*, 4240−4246. (b) Zhou, L.; Gao, C.; Xu, W.; Wang, X.; Xu, Y. *Biomacromolecules* **2009**, *10*, 1865−1874.
(16) (a) Orski, S. V.; Poloukhtine, A. A.; Arumugam, S.; Mao, L.; Popik, V. V.; Locklin, J. *J. Am. Chem. Soc.* **2010**, *132*, 11024−11026. (b) Evans, H. L.; Slade, R. L.; Carroll, L.; Smith, G.; Nguyen, Q. D.; Iddon, L.; Kamaly, N.; Stöckmann, H.; Leeper, F. J.; Aboagye, E. O.; Spivey, A. C. *Chem. Commun.* **2012**, *48*, 991−993.
(17) (a) Landfester, K. *Angew. Chem., Int. Ed.* **2009**, *48*, 4488−4507. (b) Sisson, A. L.; Papp, I.; Landfester, K.; Haag, R. *Macromolecules* **2009**, *42*, 556−559.
(18) (a) Landfester, K.; Bechthold, N.; Tiarks, F.; Antonietti, M. *Macromolecules* **1999**, *32*, 5222−5228. (b) Cao, Z.; Ziener, U.; Landfester, K. *Macromolecules* **2010**, *43*, 6353−6360.
(19) Wu, C.; Bull, B.; Szymanski, C.; Christensen, K.; McNeill, J. *ACS Nano* **2008**, *2*, 2415−2423.
(20) (a) Yu, D.; Zhang, Y.; Liu, B. *Macromolecules* **2008**, *41*, 4003−4011. (b) Jin, Y.; Ye, F.; Wu, C.; Chan, Y. H.; Chiu, D. T. *Chem. Commun.* **2012**, *48*, 3161−3163.